

# Design Optimization of Split Ring Resonator Array

Nur Ahlina Yusop and Nor Muzlifah Mahyuddin

**Abstract** Split Ring Resonator (SRR) is widely used in research area due to its compactness characteristics and low implementation cost. SRR can be incorporated with microstrip line and can be tested for various purposes. This paper, will present about the wide properties of SRR in term of different size, spacing and rejection of SRR during transmission. From the result, it shows that when the size of SRR increases, the resonance frequency decreases. This is due to the inverse relationship between the SRR dimension and the resonance frequency which also involves the inductance value. Moreover, the effect on SRR separation also will be studied. As the distance separation between SRR decreases, the coupling between SRR will be increased.

**Keywords** Split ring resonator • Microstrip line • Characteristics of SRR • Array size • Gap size

## 1 Introduction

Split Ring Resonator design has quickly raise attention among researchers where evidently several types or topologies have been developed in various applications such as CSRR, BC-SRR. Due to its negative permeability characteristics, it is also implemented in research area such as dielectric characteristics sensing area. SRR exhibits metamaterial property which acts as a resonator that split in the opposite ends of each concentric annular ring. The ring is designed in pairs which have small gap between them. Subsequently, it is made up of copper or gold [1]. The negative

---

N.A. Yusop (✉) · N.M. Mahyuddin  
School of Electrical and Electronic Engineering, Engineering Campus,  
Universiti Sains Malaysia, 14300 Nibong Tebal, Pulau Pinang, Malaysia  
e-mail: nay15\_eee010@student.usm.my

N.M. Mahyuddin  
e-mail: ee.mnmuzlifah@eng.usm.my

permeability behavior of SRR as stated by Pendry [2] can be classified as Left-Handed Metamaterial (LHM) which is known to behave like a negative index naturally [3–6]. For the basic operation of SRR, magnetic flux penetrating the metal ring will induce rotating currents in the rings. Consequently, it will produce its own flux to enhance the incident field. In addition, the small gap between the rings can produce large capacitance values. The resonant frequency and the bandwidth of the SRR can be determined by its total length and its physical width [7]. The resonance frequency resulted from the split ring resonator is much smaller than the corresponding classical ring or square loop resonators of similar dimension. This is due to large distribution capacitance between the two rings. The resonant frequency is dependable on several factors such as thickness of the ring, inner diameter, and the split gap as well as the electrical permittivity which will be explored in this paper [8].

In term of Q-factor, this metamaterial resonator carries a high Q-factor along with the small size dimension. Subsequently, due to its compactness, SRR performs better [9]. Referring to the microstrip technology, SRR can only be etched in the upper substrate side and next to the microstrip transmission line. Therefore the coupling between SRR and microstrip line can be strengthened by reducing the gap as small as possible. This paper focuses on the factor that can affect the performance of SRR. Consequently, the size of SRR remains constant. However, several parameters or configuration of SRR can be developed against the performance which includes different length of SRR, the position and the number of array added in the SRR design.

## 2 Design of Split Ring Resonator (SRR)

SRR can be included in metamaterial structure that has split at the opposite ends of each annular ring. This concentric annular ring usually is designed in pair which have small gap between the rings. Schematic diagram of split ring resonator including its parameter is shown in Fig. 1. All the details and specification of parameters are tabulated in Table 1.

However, the outer rings and the inner gap are important factors that need to be taken into consideration when designing SRR since it represents the capacitance and inductance of the SRR [10].

When microstrip line is loaded with SRR, it will produce higher Q factor and will act as bandstop filter. A better performance can be achieved when SRR array is added to microstrip transmission line as shown in Fig. 2. Width of transmission line is represented by  $w$ ; gap between transmission line and SRR represent  $b$ ; gap between SRR ring is  $a$ ;  $g$ ,  $c$  and  $d$  represent the gap, width and length of SRR respectively [12].

In this SRR array design, R04003C is used as a substrate together with 50  $\Omega$  microstrip line. The thickness of substrate is 0.813 mm with the dielectric constant

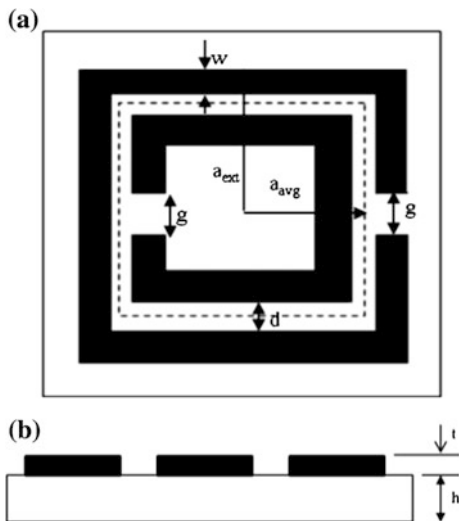


**Fig. 1** Schematic diagram of a SRR with strip of width,  $w$ , outer length,  $a_{ext}$ , inner length,  $a_{avg}$ , with ring spacing,  $d$  and split gap,  $g$ , **b** thickness of metallic strips,  $t$ , printed on dielectric substrate with thickness,  $h$  [10]

**Table 1** SRR dimension and parameters [11]

Parameter	Definition
$f_o$	Resonant frequency $\frac{1}{2\pi\sqrt{L_T C_{eq}}}$
$L_T$	Total equivalent inductance for a wire of rectangular cross section of a single SRR having finite length, $l$ and width, $w$ $0.0002l(2.303 \log_{10} \frac{4l}{w} - \gamma)\mu H$ $l = 8a_{ext} - g$
$\gamma$	Constant for a wire loop of square geometry, 2.853
$C_{eq}$	Total equivalent capacitance with series capacitance, $C_o$ and gap capacitance, $C_g$ $\frac{(C_o + C_g)}{2}$
$C_o$	$(4a_{avg} - g)C_{pul}$
$a_{avg}$	$a_{ext} - w - d/2$
$C_{pul}$	Capacitance per unit length $\sqrt{\epsilon_r}/c_o Z_o$
$Z_o$	Characteristic impedance, 50 $\Omega$
$c_o$	Velocity of light in free space, $3 \times 10^8$
$C_g$	$\frac{\epsilon_o w t}{g}$

of 3.38. Figure 3 shows the side view of SRR design includes 50  $\Omega$  transmission line with a width of 1.8653 mm. In this design, the substrate has been laminated with 0.035 mm of copper layer. Table 2 shows the dimension of SRR used in this work.

**Fig. 2** Schematic view of SRR coupled to a transmission line

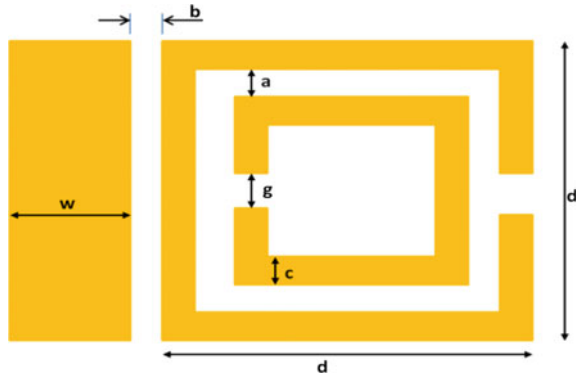


**Fig. 3** Side views of SRR with its parameters and dimensions

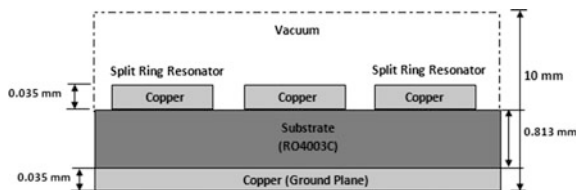


**Table 2** Dimension of SRR

Parameter	Dimension (mm)
Gap between transmission line and SRR, <i>b</i>	0.3
Gap between ring of SRR, <i>a</i>	0.3
Width of ring of SRR, <i>c</i>	0.5
Length of SRR, <i>d</i> ( <i>d</i> is varies in this experiment)	4.6, 4.8, 5.0

### 3 Distance Separation Between Each SRR

The dimension of SRR is calculated based on the resonant frequency at 5.8 GHz. The first factor that can be discovered that can be taken into consideration when designing SRR is the distant separation between each array of SRR. In this part, the length of the SRR, *d*, is being fixed for its value. The only parameter that has been manipulated is the distance between SRR (*s*). Tzong-Lin Wu on his Microwave Filter Design lecture stated that the distance between each resonator as  $\lambda/4$ . The value of wavelength  $\lambda_g$  can be obtained by using Eq. 1 [13].

$$\lambda_g = \frac{c}{\sqrt{\epsilon_r}f} \tag{1}$$

Where;

- c = speed of light,  $3 \times 10^8$
- $\epsilon_r$  = dielectric constant of a substance, 3.38
- f = resonant frequency, 5.8 GHz

$$\lambda_g = \frac{(3 \times 10^8)}{(\sqrt{3.38})(5.8G)}$$

$$\lambda_g = 0.02813$$

After obtaining the value of  $\lambda_g$ , three different distances between SRR, s have been decided to be tested which are  $\lambda_g/2$ ,  $\lambda_g/4$ ,  $\lambda_g/6$ . The length of SRR is fixed to 4.6 mm for all three simulations whereas the distance is varied accordingly. The schematic diagram and the results of simulation for three different distance of SRR are shown in Fig. 4.

As illustrated in Fig. 4, then the separation distance between SRR ( $d$ ), decreases from  $\lambda/2$  to  $\lambda/4$ , the coupling increases and the transmission spectrum of microstrip line falls to  $-7.461$ – $-13.12$  dB. For a shorter separation which is  $\lambda/6$ , two resonances appear [14].

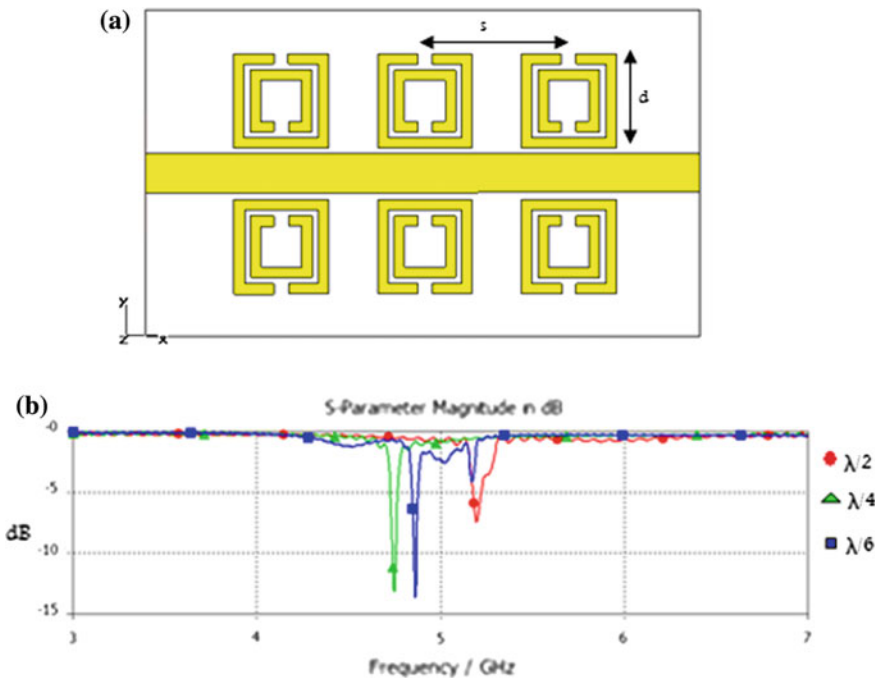


**Fig. 4** Split Ring Resonator (SRR) along with microstrip line shows the distance separation, s and side length of each SRR, d, in (a) and transmission spectrum of microstrip line for distance  $\lambda/2$ ,  $\lambda/4$ , and  $\lambda/6$  (b)

### 4 Implementation of SRR with Different Side Length and Array Configuration

In this part, the SRR are being used and the properties of SRR in term of distance, length of SRR are being varied and analysed. By referring to schematic diagram in Fig. 4a, SRR are being tested with different value of side length of SRR ( $d$ ) and the rejection of frequency resonant of SRR is observed. The distance separation between each SRR,  $s$ , is fixed to  $\lambda/4$ . Three different lengths of SRR are sketched which are 4.6, 4.8 and 5.0 mm. In this case, the substrate is a 1.89 mm-thickness of Roger 4003. Figure 5 will show the simulation result for three different length of SRR used.

The observations have been made based on the value of the rejection when the array of SRR was added onto the design. Some observations also have been made on the changes of resonance frequency when different length of SRR is used. Table 3 shows the result for this simulation.

Three different lengths of SRR are tested for a single array of SRR as shown in Fig. 5. From the Table 3, it can be concluded that if the side length of SRR or the size of the rings increases, the resonance frequency will decrease.

$$f_o = \frac{1}{2\pi\sqrt{L_T C_{eq}}} \tag{2}$$

$$a_{ext} = a_{avg} + w + d/2 \tag{3}$$

Where;

$L_T$  = Total equivalent inductance

$C_{eq}$  = Total equivalent capacitance

From Eq. 2, the total equivalent inductance,  $L_T$  is inversely proportional to the frequency. By referring back to Table 1, the equation of  $L_T$  includes  $l$  and  $w$  parameters which represent length and width of SRR. For the  $l$  equation, it incorporates  $a_{ext}$  as a part of its equation which is shown in Eq. 3. Therefore, from Eq. 3, it clearly can be seen that the length of SRR which is represented by  $d$  can influence

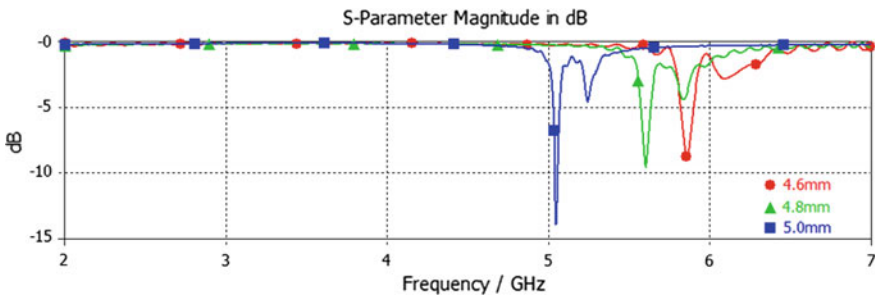


Fig. 5 Transmission spectrum of SRR array when  $d$  is 4.6, 4.8 and 5.0 mm

**Table 3** Result summary of 3 different length for a single SRR array

Length, d(mm)	Centre Freq. (GHz)	$S_{11}$ (dB)
4.6	5.86	-8.873
4.8	5.61	-9.525
5.0	5.05	-13.91

$a_{ext}$ . The SRR dimension represented by  $d$  and  $a_{ext}$  are directly proportional to  $L_T$  which indicates any increase in the  $d$  or  $a_{ext}$  will increase  $L_T$ , thus decreasing the resonance frequency as shown in the illustrated results.

## 5 Conclusions

When implementing SRR into microstrip line, if more than one SRR cell is being used, the distance of separation between each SRR can be neglected. The small changes can be considered insignificant. Distance of  $\lambda/4$  is widely used by researchers when working with SRR. The relation between the lengths of SRR with frequency rejection can be clearly seen in this work. Therefore, it can be concluded that if the size of the SRR rings increases, the resonance frequency will decrease.

**Acknowledgments** I would like to express my acknowledgement to Universiti Sains Malaysia for providing financial support by Research University Grant (1001/PELECT/814206) for this research.

## References

1. Al-Nuaimi MKT, Whittow WG (2010, April). Compact microstrip band stop filter using SRR and CSSR: design, simulation and results. In: Proceedings of the fourth european conference on antennas and propagation (EuCAP), 2010, 1–5. IEEE
2. Pendry JB, Holden AJ, Robbins DJ, Stewart WJ (1999) Magnetism from conductors and enhanced nonlinear phenomena. *IEEE Trans Microw Theory Tech* 47(11):2075–2084
3. Smith DR, Padilla WJ, Vier DC, Nemat-Nasser SC, Schultz S (2000) Composite medium with simultaneously negative permeability and permittivity. *Phys Rev Lett* 84(18):4184
4. Pendry JB, Holden AJ, Stewart WJ, Youngs I (1996) Extremely low frequency plasmons in metallic mesostructures. *Phys Rev Lett* 76(25):4773
5. Veselago VG (1968) The electrodynamics of substances with simultaneously negative values of  $\epsilon$  and  $\mu$ . *Phys Usp* 10(4):509–514
6. Shelby RA, Smith DR, Schultz S (2001) Experimental verification of a negative index of refraction. *Science* 292(5514):77–79
7. Fallahzadeh S, Bahrami H, Tayarani M (2009) A novel dual-band bandstop waveguide filter using split ring resonators. *Prog Electromagn Res Lett* 12:133–139
8. Wu B, Li B, Su T, Liang CH (2006) Study on transmission characteristic of split ring resonator defected ground structure. *Prog Electromagn Res* 50:710–714
9. Al-Naib IA, Jansen C, Koch M (2009) High Q-factor metasurfaces based on miniaturized asymmetric single split resonators. *Appl Phys Lett* 94(15):153505

10. Mahyuddin NM, Kadir NFSA (2014, January). Design of a 5.8 GHz bandstop filter using split ring resonator array. In: The 8th International conference on robotic, vision, signal processing & power applications, 473–482. Springer Singapore
11. Saha C, Siddiqui JY, Antar YM (2011, August). Square split ring resonator backed coplanar waveguide for filter applications. In: 2011 XXXth URSI general assembly and scientific symposium, 1–4
12. Öznazl V, Erturk VB (2013) On the use of split-ring resonators and complementary split-ring resonators for novel printed microwave elements: simulations, experiments and discussions. Bilkent University
13. Pozar DM (2009) Microwave engineering. John Wiley & Sons
14. Gay-Balmaz P, Martin OJ (2002) Electromagnetic resonances in individual and coupled split-ring resonators. *J Appl Phys* 92(5):2929–2936